UCID- 16776

Lawrence Livermore Laboratory

NUMERICAL RESULTS FROM A STUDY OF LiH: THE PROPOSED STANDARD MATERIAL FOR THE HIGH PRESSURE SHOCK EXPERIMENT

F. J. Rogers

May 6, 1975

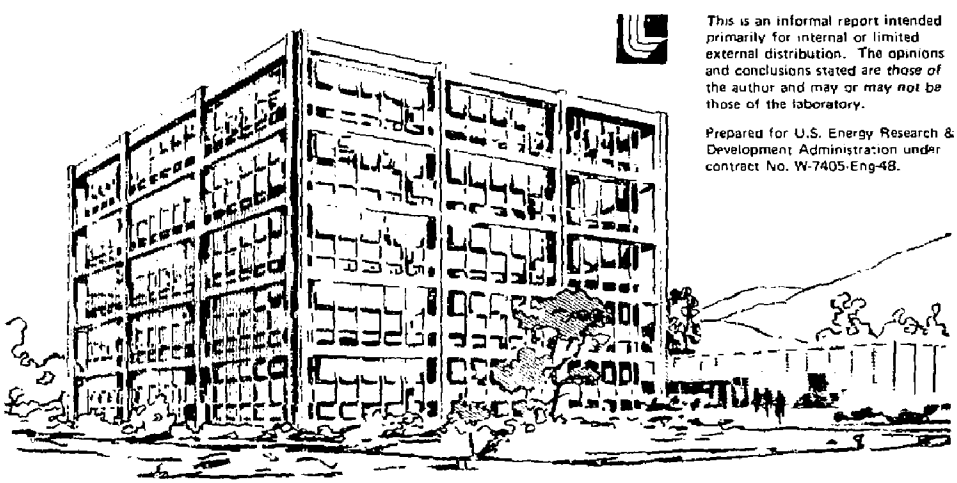

Prepared for U.S. Energy Research & Development Administration under contract No. W-7405-Eng-48.

NUMERICAL RESULTS FROM A THEORETICAL STUDY OF LiH: THE PROPOSED STANDARD EOS TABLE FOR THE HIGH PRESSURE SHOCK EXPERIMENT

INTRODUCTION

What is the Experiment?

It is proposed to send a high pressure shock wave through a layer of LiH and then into a sample of high Z-material, resulting in a reflected shock wave back into the LiH. If the Hugoniot and some reflected Hugoniots for LiH are known the EOS of the sample can be obtained from the "impedance matching method."

What is the Value of the Experiment?

The EOS in the 20-250 Mbar pressure range, with temperatures in the range 20-100 eV, can be measured. Moreover, this is the least understood range of the EOS because:
(1) The Thomas-Fermi theory is not expected to be very accurate in this range.
(2) It is very difficult to access this region experimentally and only a few experiments of uncertain accuracy have been performed.[1]

How is the EOS of LiH to be Obtained?

Over a several year period there has been an H Division effort to develop the theory and computational capability for obtaining the EOS of incompletely ionized plasmas. The procedure is to work directly from the Coulomb law of force between the electrons and bare nuclei in the plasma and apply the first principles of quantum statistical mechanics. The result of this effort is a theory that allows one to systematically add plasma interaction terms beyond those commonly referred to as "Debye-Hückel corrections," while at the same time accounting for the formation of composite ions, atoms, and molecules in the plasma.

The theory developed is in principle applicable to any material. However, because of the detailed nature of the calculations, i.e., the calculation of screened energy levels and interaction potentials for the composite particles, it is much easier to work with low-Z materials. LiH is chosen because it represents a good compromise between calculational difficulty and a reasonably high shock impedance.

SUMMARY OF THE THEORY AND ITS RANGE OF VALIDITY

Figure 1 gives schematically the steps involved in the theoretical development. One additional step, not explicitly treated in Refs. 3,4 is required to bring the theoretical description up to the level actually used in numerical calculations. That is to go back to step (3) and introduce degeneracy modifications to $P/kT = f(S)$ and then repeat steps (4) and (5).

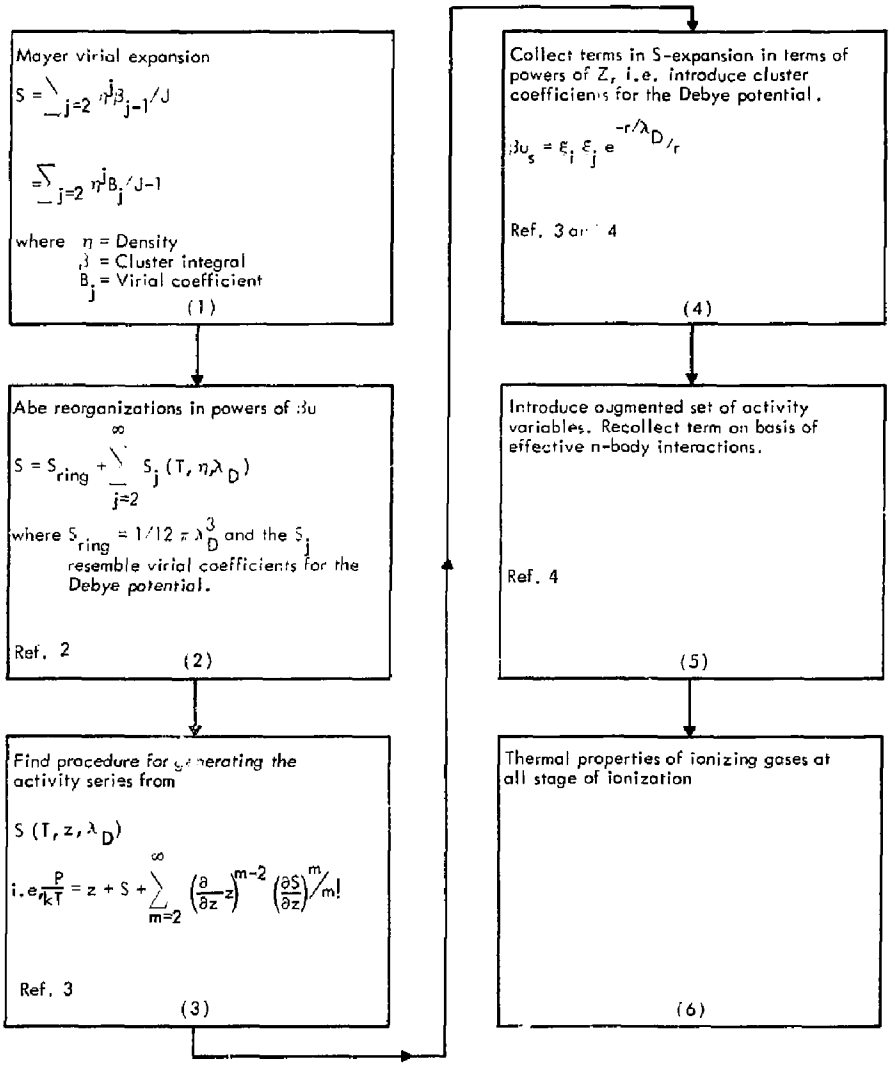

Fig. 1. Steps involved in the theoretical development of the EOS.

A numerical description of how the eigenvalues and phase shifts for the screened coulomb potential were calculated is given in Refs. 5,6. The interest in the present communication is not in theoretical development, but in the reporting of numerical calculations and their range of validity. Since experimental data is nonexistent it is necessary to look elsewhere to determine the range of validity of the theory.

The Brush, Sahlin and Teller (BST) Monte Carlo calculation[4] for a classical one-component plasma in a uniform background is essentially an "exact" result for such a system. A comparison of the classical activity expansion with BST will give some insight into its convergence properties. This comparison is shown in Fig. 2, where $\Lambda = \hbar e^2/\lambda_D$ (λ_D = Debye length). Curve A includes terms in $z^{5/2}$ (z = activity) and is equivalent to the Debye-Hückel correction. Curve B includes all terms through $z^{5/2}$. It is seen that the three curves move sequentially further out on the BST curve, indicating that the $z^{5/2}$ expansion is a significant improvement over the Debye-Hückel theory. (For additional details see Appendix C of Ref. 5.)

The BST calculation applies only to real plasmas that are completely ionized and in which the electrons are very degenerate. Neither of these conditions apply in the density-and-temperature range of current interest and one might at first think the above comparison to be irrelevant. However, the major complication in the convergence of the activity series is due to the long range of the coulomb potential and it is just this aspect of the problem that is being compared in the above example.

For real plasmas the reason that classical theory cannot be applied lies in the strong attractions between electrons and nuclei. This effect can be handled in classical theory by modifying the 1/r form of the potential at short distances to take account of the uncertainty principle leaving the long range part of the problem unaltered. In view of this, we expect the convergence of the quantum activity expansion to be similar to that of the classical activity expansion provided that: (1) The ratio of the de Broglie wavelength to Debye length is small; (2) The electrons are not very degenerate.

Figure 2 shows the convergence of the activity series in the case that a numerically accurate result is known. Since no rigorous theoretical or experimental result exists for real multicomponent plasmas, however, convergence criteria will be based on the convergence of the classical one-component gas.

If we group the terms in curve C according to their leading z-dependence it is found that all coefficients are positive. In an ordinary series if $U_{m+1}/U_m \leq 1/2$ the maximum error in the series is equal to the last term kept. However, because of the density constraint, i.e.,

$$n = z \frac{\partial (P/kT)}{\partial z} \quad ,$$

the activity is a function of the number of terms in the expansion. When the coefficients are all positive the activity decreases each time an additional term is kept and the pressure decreases, irrespective of the fact that the terms in the pressure expansion are all positive.

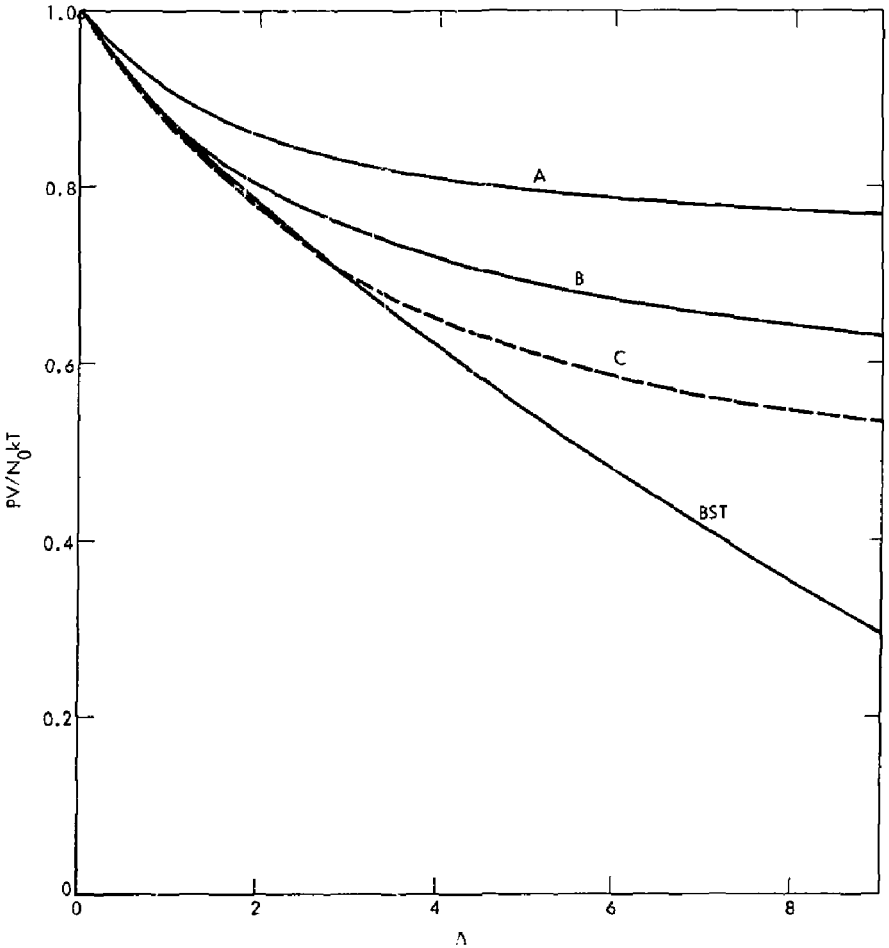

Fig. 2. Comparison between classical activity expansion truncated to various orders and the BST Monte Carlo calculation for a one-component plasma.

It is observed that a reasonable estimate of the maximum error in the pressure is given by the negative of the last term kept, at least, in the $z^{5/2}$ expansion. A less conservative estimate of the error can be obtained by extrapolating P/kT as a function of the number of terms retained in the expansion. This is also the most convenient method of estimating the error in the energy. (In the classical case the energy can be obtained easily from the virial theorem.)

In this communication attention will be given exclusively to that part of density-temperature space traversed by the Hugoniot and reflected Hugoniots. Once the equation of state is calculated the Hugoniot curve can be obtained by finding the zeros of

$$H(\varepsilon,T) = E(\varepsilon,T) - E_{OH} - \frac{1}{2}(V_{OH} - V)(P + P_{OH}) \qquad (1)$$

where

ε = density
T = temperature
E_{OH} = initial energy of sample
P_{OH} = initial pressure of sample
V_{OH} = initial volume.

Reflected Hugoniots can be obtained from an expression similar to Eq. (1) except E_{OH} and P_{OH} are replaced with E_I and P_I, i.e., the energy and pressure attained by the initial shock.

Some Hugoniots and reflected Hugoniots obtained from ACTEX, the computer code that implements the theory outlined in Fig. 1, are plotted in Fig. 3. The reflected Hugoniots are labeled R1, R2, R3, and R4, respectively. The 20-eV, 30-ev, 40-ev, and 50-eV isotherms are plotted as dashed lines. The 2% and 5% maximum pressure error curves, based on the size of the last terms calculated, are also shown. The 2% curve is seen to cross the Hugoniot at 135 mbar, whereas, the 5% curve crosses at 32 mbar. Furthermore, the 2% uncertainty curve rises much faster with increasing density than the 5% curve. There are two reasons for this: (1) The 2% curve lies in a region where the gas is almost completely ionized, whereas the 5% curve lies in a region where Li^{++} and Li^{+} have formed, thus reducing the number of ions and their Coulomb interaction. (2) Even though there are fewer free electrons along the 5% curve they are more degenerate. Since degeneracy improves the convergence of the activity series, compared to a Boltzmann gas, this effect also helps to prevent the errors from increasing rapidly as the temperature is reduced.

The calculations presented in Fig. 3 are strictly only valid when $\gamma = \lambda/\lambda_D$ (λ = de Broglie wavelength, λ_D = Debye length) is small and when the electron degeneracy parameter, μ/kT, is negative. Reasonable limits for these parameters appear to be $\gamma = 0.7$ and $\mu/kT = -0.5$. The $\gamma = 0.7$ curve is plotted in Fig. 3. The $\mu/kT = -0.5$ curve is not plotted but lies fairly close to the $\gamma = 0.7$ curve.

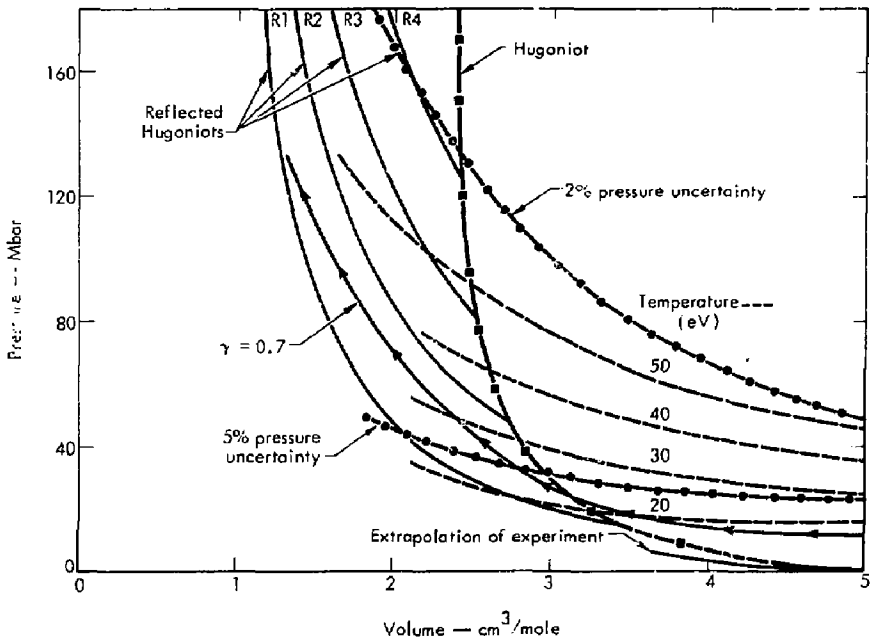

Fig. 3. Hugoniots and reflected Hugoniots obtained from ACTEX, based on theory outlined in Fig. 1.

Since the main item of interest in the current paper is the Hugoniot and reflected Hugoniots it is of interest to see how well the $z^{5/2}$ activity expansion has converged on the location of these curves. To do this we start with an expansion that includes only terms of order z, i.e., the Saha equation, and calculate the Hugoniot curves. Next we add the terms of order $z^{3/2}$, i.e., the Debye-Hückel correction, and calculate a new set of Hugoniots. This process is repeated for the z^2 and $z^{5/2}$ terms. The results for the Hugoniot and one reflected Hugoniot are shown in Fig. 4. The change in the location of the reflected Hugoniot curve in going from the Saha equation to the Saha equation with Debye-Hückel corrections is large, approximately 23% shift in pressure at a given volume, whereas the change in going from the $z^{3/2}$ curve to the $z^{5/2}$ curve is much smaller, approximately 3% in pressure at a given volume. The z^2 curve lies quite close to the $z^{5/2}$ curve and has not been plotted. This indicates that, provided the treatment of diffraction and degeneracy corrections in the present theory are adequate, the Hugoniot curves are accurately located by the $z^{5/2}$ expansion.

The most important plot for analyzing experimental data by the impedance-matching method is a $P\text{-}U_p$ plot. This is given for LiH in Fig. 5. The volumes along the Hugoniot indicate the volumes at which the reflected Hugoniots originate. Also plotted is the $P\text{-}U_p$ obtained from a linear extrapolation of the experimental $U_s\text{-}U_p$. It is seen that the theoretical $P\text{-}U_p$ curve matches up smoothly with the experimental curve.

Figure 6 is a replot of the left half of Fig. 5 for the purpose of making an error analysis. The lead Hugoniot of Trunin et al.[2] is used as an example to assess the errors in the "impedance matching procedure." Even though the Hugoniots obtained with expansion of different orders are spread out in the P-V plane, there is very little spread in the $P\text{-}U_p$ plane. In fact the $z^{3/2}$ and $z^{5/2}$ expansions are indistinguishable and the z expansion lies only slightly higher than these two.

The TFCMIX Hugoniot also lies close to the ACTEX curves. Even though the $z^{3/2}$ and $z^{5/2}$ Hugoniots are indistinguishable their reflected Hugoniots separate slightly as indicated by the increased thickness of line for the middle reflected Hugoniot. An example of the separation of the z expansion and $z^{5/2}$ expansion is indicated for the highest-lying reflected Hugoniot.

With a knowledge of $P\text{-}U_p$ for LiH the pressure in Pb can be obtained by a measurement of the shock velocity in LiH, U_{s1}, and the shock velocity in lead, U_{s2}. The intersection of a straight line of slope $\rho_{LiH}\ U_{s1}$, emanating from the origin, with the $P\text{-}U_p$ curve of LiH locates the foot of the reflected Hugoniot whose pressure and particle velocity has to match that of the Pb Hugoniot. The intersection of a straight line of slope $\rho_{Pb}\ U_{s2}$, emanating from the origin, with the reflected Hugoniot determines the pressure and particle velocity at the interface. This graphical solution is shown in Fig. 6. The curves drawn are for $U_{s1} \pm 2\%$ and $U_{s2} \pm 2\%$. This introduces an error in the pressure of ±3.3% and of approximately ±4.3% in U_p. However, the percentage error in the density of the Pb is much larger. Consider the ratio

$$\frac{\rho}{\rho_0} = \frac{V_0}{V} = \frac{1}{1 - \frac{V_0 - V}{V_0}} = \frac{1}{1 - \frac{U_p}{U_s}} \qquad (2)$$

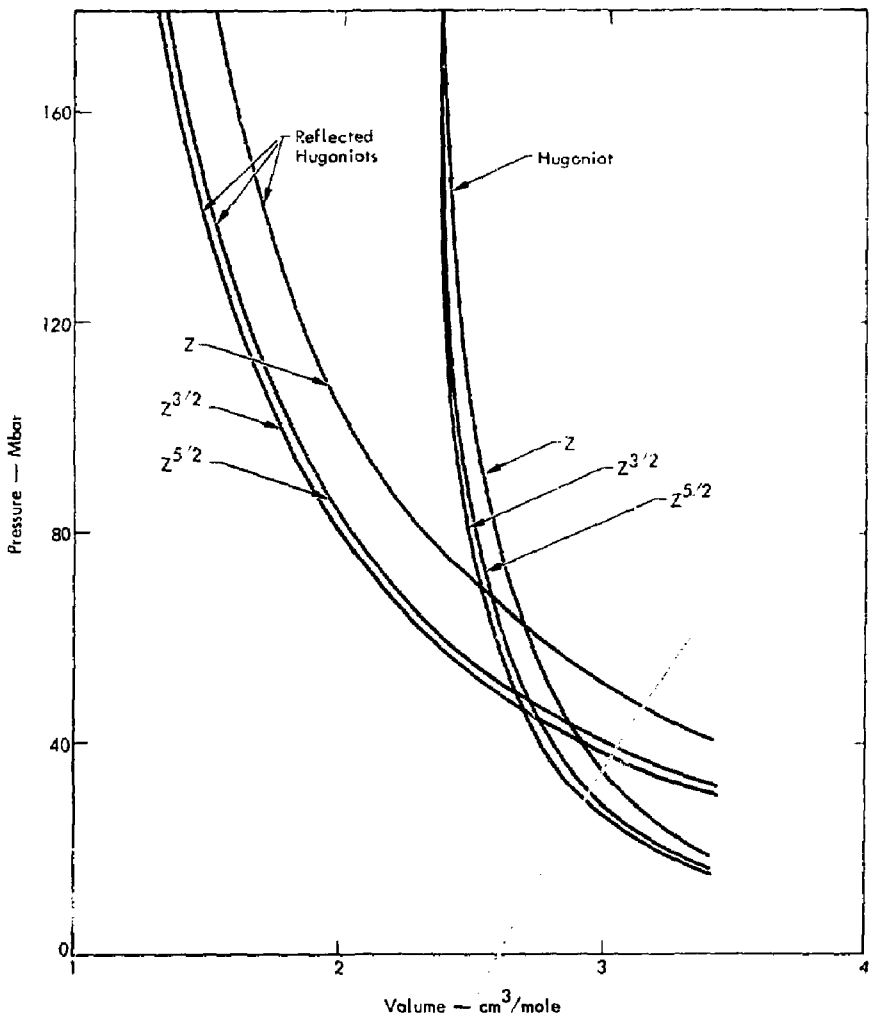

Fig. 4. Successive approximations to the Hugoniot and reflected Hugoniot to show the convergence obtained by adding higher-order terms.

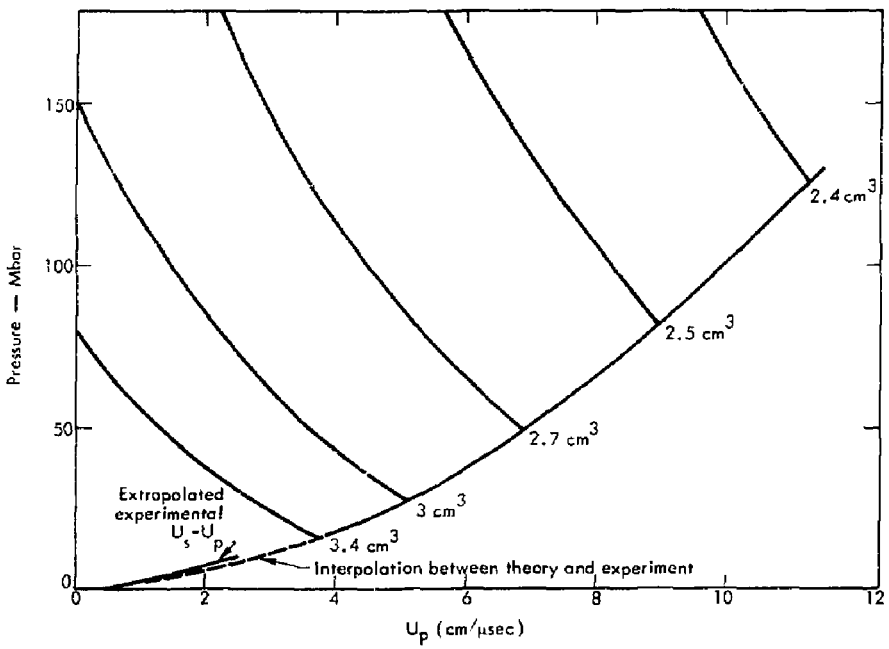

Fig. 5. Comparison between theoretical and experimental pressure vs particle velocity curves for LiH.

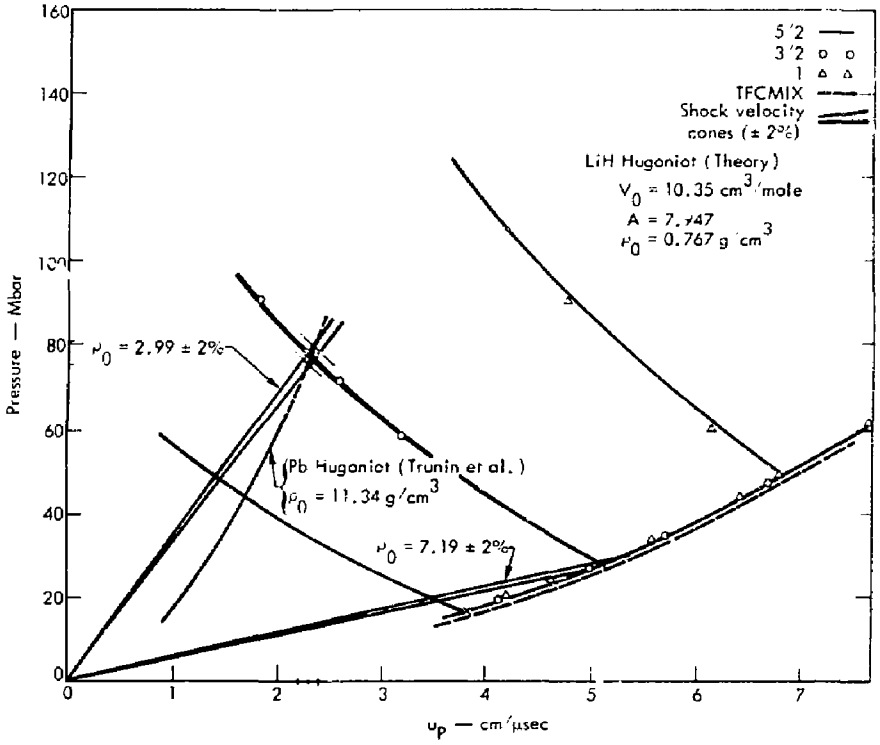

Fig. 6. Replot of Fig. 5 left half, showing error analysis.

where the right-hand side comes from a substitution of the Hugoniot relations. Taking the differential of Eq. (2) we get

$$\frac{\Delta\rho}{\rho_0} = -\frac{\Delta(U_p/U_s)}{\left(1 - \frac{U_p}{U_s}\right)^2} \quad . \tag{3}$$

Division by $\Delta U_p/U_s$ gives

$$\frac{\Delta\rho}{\rho_0} = \frac{1}{\frac{U_s}{U_p} - 1} \quad \frac{\Delta(U_p/U_s)}{(U_p/U_s)} \quad . \tag{4}$$

Substitution of the values from Fig. 1 gives, after division by U_p/U_s,

$$\frac{\Delta\rho}{\rho_0} = \frac{1}{\frac{2.99}{2.13} - 1} \quad \left(\frac{1 \pm 0.0045}{1 \mp 0.02} - 1\right) \approx 0.15\% \text{ r.s.} \quad .$$

This example underlines the fact that the shock velocity measurements must be very accurate if an accurate EOS point is to be obtained.

The calculations presented in this paper were based on a first-principles quantum-statistical treatment of coulomb interactions. Nevertheless, because of the complexity of the theory we have found it necessary to make some approximations with regard to quantum diffraction and electron degeneracy in a region where the error due to these approximations should be small. This is an area of active theoretical study and revisions of this document will be issued as new refinements are coded into ACTEX.

ACKNOWLEDGMENT

Thanks are due to Glen Huggin for his assistance in developing the ACTEX code and for carrying out the numerical calculations presented in this report. The author also thanks Richard Grover for many useful discussions.

REFERENCES

1. R. F. Trunin, M. A. Podurets, B. N. Moiseev, G. V. Simakov, and L. V. Popov, Sov. Phys. JETP 29, 630 (1969), ibid 35, 550 (1972), Physics of the Solid Earth (1971), p. 8.
2. R. Abe, Prog. Theor. Phys. 22, 213 (1959).
3. F. J. Rogers and H. E. De Witt, Phys. Rev. A8, 1061 (1973).
4. F. J. Rogers, Phys. Rev. A10, 2441 (1974).
5. F. J. Rogers, H. C. Graboske, Jr., and D. J. Harwood, Phys. Rev. A1, 1577 (1970).
6. F. J. Rogers, Phys. Rev. A4, 1145 (1971).
7. S. G. Brush, H. L. Sahlin, and E. Teller, J. Chem. Phys. 45, 2102 (1966).

RBC/lt

Printed in the United States of America
Available from
National Technical Information Service
U. S. Department of Commerce
5285 Port Royal Road
Springfield, Virginia 22151
Price: Printed Copy $___*; Microfiche $2.25

*Pages	NTIS Selling Price
1-50	$4.00
51-150	$5.45
151-325	$7.60
326-500	$10.60
501-1000	$13.60